Memoirs of the Faculty of Engineering, Okayama University, Vol.35, Nos.1&2, pp.63-75, March 2001

Nonorthogonal Tight-Binding Molecular Dynamics for $Si_{1-x}Ge_x$ *Alloys*

Shigeru SHINOMIYA*, Chieko TOTSUJI**, Kenji TSURUTA**,
and Hiroo TOTSUJI**

(Received December 19, 2000)

We present a theoretical study of $Si_{1-x}Ge_x$ alloys based on tight-binding molecular dynamics (TBMD) calculations. First, we introduce a new set of nonorthogonal tight-binding parameters for silicon and germanium based on the previous work by Menon and Subbaswamy [Phys. Rev. B **55**, 9231 (1997); J. Phys: Condens. Matter **10**, 10991 (1998)]. We then apply the method to structural analyses of $Si_{1-x}Ge_x$ alloys. The equilibrium volume and atomic structure for a given x are obtained by the TBMD method. We also calculate the bulk modulus B, elastic constants C_{11}, C_{12} and C_{44} as a function of x. The results show that the moduli vary monotonically, but nonlinearly, between the values of Si crystal and Ge crystal. The validity of the results is also discussed.

1 INTRODUCTION

Recently, silicon/germanium interface and their mixture play important roles in many semiconductor devices. It has been known that SiGe alloys or superlattices have promising properties for the optical applications where bulk crystals cannot be directly used because of the in-direct energy gap in their electronic structures. The major problem in fabricating these materials is the mechanical stability of the alloy structure and interfaces. Understanding the structural and elastic properties of SiGe alloys and superlattices is therefore important for development of new optical materials. Tight-binding molecular dynamics (TBMD) simulation is a powerful method to investigate theoretically structural and electronic properties of semiconducting materials and interfaces.

In this paper, we present nonorthogonal tight-binding calculations for $Si_{1-x}Ge_x$ alloys. The computational efficiency of the tight-binding method over the other methods, such as those based on the density-functional theory, derives from an empirical parametrization of the single-electron Hamiltonian. Incorporation of the nonorthogonality of the orbitals allows better description of the structural properties compared to the orthogonal tight-binding approximation [1]. In the present study we report an approach proposed by Menon and Subbaswamy [2-8], and we modify their TB parametrization of silicon and germanium with paying attention to the position of the lowest conduction band. Using these parameters we perform TBMD simulations to investigate minimum-energy structures and mechanical properties of $Si_{1-x}Ge_x$ alloys with various values of x.

This paper is organized as follows. In Sec. 2, we describe the basic methodology used in the present study. In Sec. 3, we obtain relaxed structures and their characters of $Si_{1-x}Ge_x$ alloys using the TBMD method. We then calculate elastic constants as a function of Ge content x. Finally, conclusions are given in Sec. 4.

---

*Graduate School of Natural Science and Technology
**Department of Electrical and Electronic Engineering

2 METHODS

2.1 Nonorthogonal Tight-Binding Hamiltonian

Given the basic formulation of the TB method in Appendix A, we begin with matrix elements of a hypothetical orthogonal tight-binding Hamiltonian:

$$V_{\lambda\lambda'\mu}(\mathbf{r}) = v_{\lambda\lambda'\mu} e^{-\alpha(r-d_0)}, \tag{1}$$

where $V_{\lambda\lambda'\mu}$ is the matrix element for orbitals of type λ and λ' (s or p in the present case), μ is the type of overlap configuration (σ or π), and d_0 is the bond length at an equilibrium volume.

In the extended Hückel theory [9], the relationship between the parameters characterizing the elements of the overlap matrix, $T_{\lambda\lambda'\mu}$, and the elements of an orthogonal Hamiltonian $V_{\lambda\lambda'\mu}$ is given as

$$T_{\lambda\lambda'\mu}(\mathbf{r}) = \frac{2V_{\lambda\lambda'\mu}(\mathbf{r})}{K(\mathbf{r})(\varepsilon_\lambda + \varepsilon_{\lambda'})}. \tag{2}$$

$K(\mathbf{r})$ is the Hückel nonorthogonal coefficient, and we take a simple expression as

$$K(\mathbf{r}) = K_0 e^{\sigma(r-d_0)^2}. \tag{3}$$

The Hamiltonian matrix element $H^{\mathbf{k}}_{i\alpha j\beta}$ (expressed in the nonorthogonal basis) is written by

$$H^{\mathbf{k}}_{i\alpha j\beta} = \sum_{\mathbf{L}} e^{i\mathbf{k}\cdot(\mathbf{R}_i - \mathbf{R}_j - \mathbf{L})} E_{i\alpha j\beta} \left[1 + \frac{1}{K} - {T_2}^2\right], \tag{4}$$

where i and j are atom indices and α and β are orbital indices (s, p_x, p_y, p_z). $E_{i\alpha j\beta}$ is a hypothetical orthogonal matrix element. Here, the function

$$T_2 = \frac{T_{ss\sigma}(\mathbf{r}) - 2\sqrt{3}T_{sp\sigma}(\mathbf{r}) - 3T_{pp\sigma}(\mathbf{r})}{4} \tag{5}$$

describes the overlap between two sp^3 hybrids, which depends on interatomic distance implicitly through the $T_{\lambda\lambda'\mu}$ terms.

The total potential energy of the system is given by the sum

$$E_{pot} = E_{bs} + E_{rep} + E_0, \tag{6}$$

where E_{bs} is the sum of the one-electron energies E_n for the occupied states:

$$E_{bs} = \sum_n^{occ} E_n, \tag{7}$$

(n is the band index) and E_{rep} is given by a repulsive pair potential:

$$E_{rep} = \sum_i \sum_{j>i} \phi(r_{ij}), \tag{8}$$

which accounts for the core-core repulsion and double counting of the electron-electron interaction in E_{bs}. Here r_{ij} is the separation of atoms i and j. $\phi(r_{ij})$ is modeled to be short-ranged and dependent exponentially on distance:

$$\phi(\mathbf{r}) = \phi_0 e^{-\beta(r-d_1)}. \tag{9}$$

E_0 is a constant that merely shifts the zero of the energy.

In molecular-dynamics simulations, one needs to calculate the interatomic forces exerted on each atom by

$$\mathbf{F} = -\frac{\partial E_{pot}}{\partial \mathbf{r}} = -\left(\frac{\partial E_{bs}}{\partial \mathbf{r}} + \frac{\partial E_{rep}}{\partial \mathbf{r}}\right), \tag{10}$$

where $-\frac{\partial E_{bs}}{\partial \mathbf{r}}$ is an electronic contribution to the atomic force calculated through the Hellmann-Feynman theorem (Appendix B), and $-\frac{\partial E_{rep}}{\partial \mathbf{r}}$ is the repulsive force between atoms given by

$$\frac{\partial E_{rep}}{\partial x} = -\beta\frac{x}{r}E_{rep}, \quad \frac{\partial E_{rep}}{\partial y} = -\beta\frac{y}{r}E_{rep}, \quad \frac{\partial E_{rep}}{\partial z} = -\beta\frac{z}{r}E_{rep}. \tag{11}$$

2.2 Tight-Binding Parameters for Si and Ge

In Table 1, we list all the TB parameters for Si and Ge in the present study. These parameters are obtained by modifying Menon-Subbaswamy's parameters [2-6]. The modifications are done so that the position of the lowest conduction band, lattice constants at the equilibrium volume, the total energy and elastic constants agree approximately with experimental data. The energy bands of bulk crystal of Si and Ge are shown in Fig. 1. These band structures show better form of conduction band than the original [4], although they have larger band gap than experimental band structures.

The bonding parameters between Si and Ge are assumed to be the average values of Si-Si and Ge-Ge Hamiltonian matrix elements.

Table 1: Tight-binding parameters of Si and Ge.

		Si	Ge
ε_s	[eV]	-13.55	-14.38
ε_p	[eV]	-6.52	-6.360
$v_{ss\sigma}$	[eV]	-3.20	-2.214
$v_{sp\sigma}$	[eV]	2.52	2.355
$v_{pp\sigma}$	[eV]	3.80	3.097
$v_{pp\pi}$	[eV]	-1.07	-0.998
d_0	[Å]	2.35	2.44
α	[Å^{-1}]	1.62	1.604
σ	[Å^{-2}]	2.5	1.8
K_0		1.7	1.5
β	[Å^{-1}]	8.9424	6.5956
d_1	[Å]	2.255	2.42
ϕ_0	[eV]	0.41	0.22

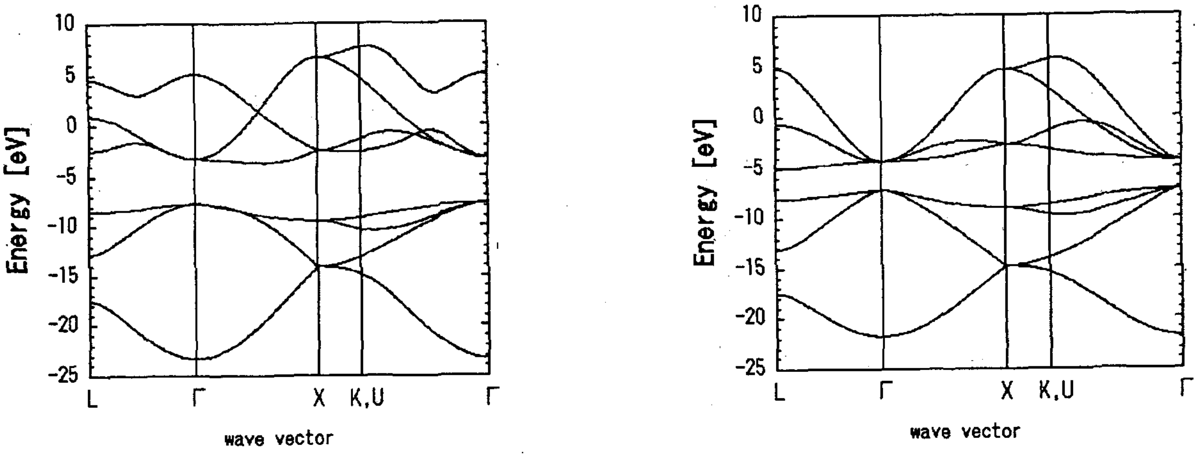

(a) (b)

Figure 1: Band structure of the diamond-structured semiconductors; (a) silicon, (b) germanium.

3 RESULTS AND DISCUSSION

3.1 Relaxed Structures of $Si_{1-x}Ge_x$

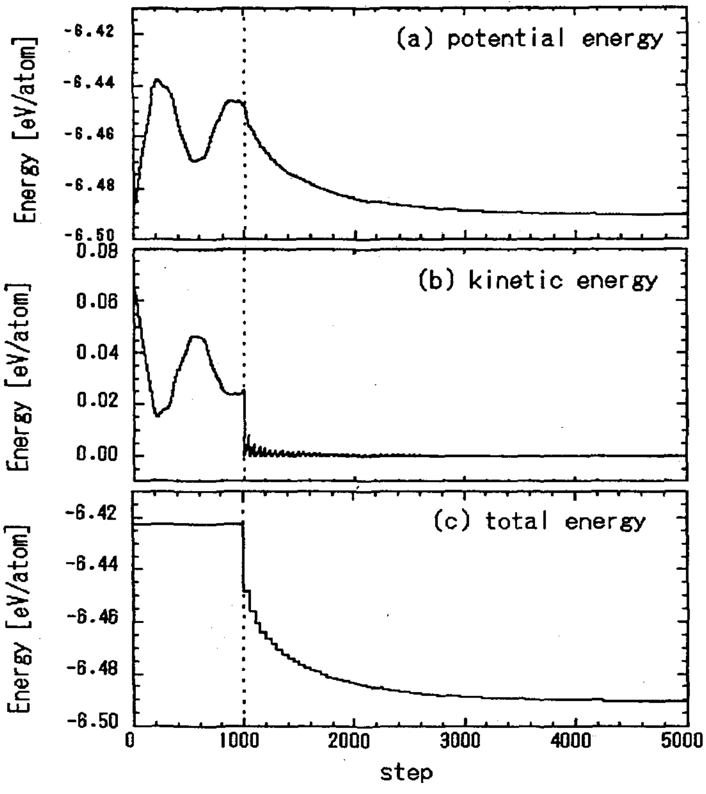

Figure 2: Time evolution of (a) potential energy, (b) kinetic energy and (c) total energy in the relaxation processes using TBMD method. Starting at a temperature 500 K, the system is annealed for first 1000 MD steps. After 1000 steps, the system is quenched by removing kinetic energy every 50 step.

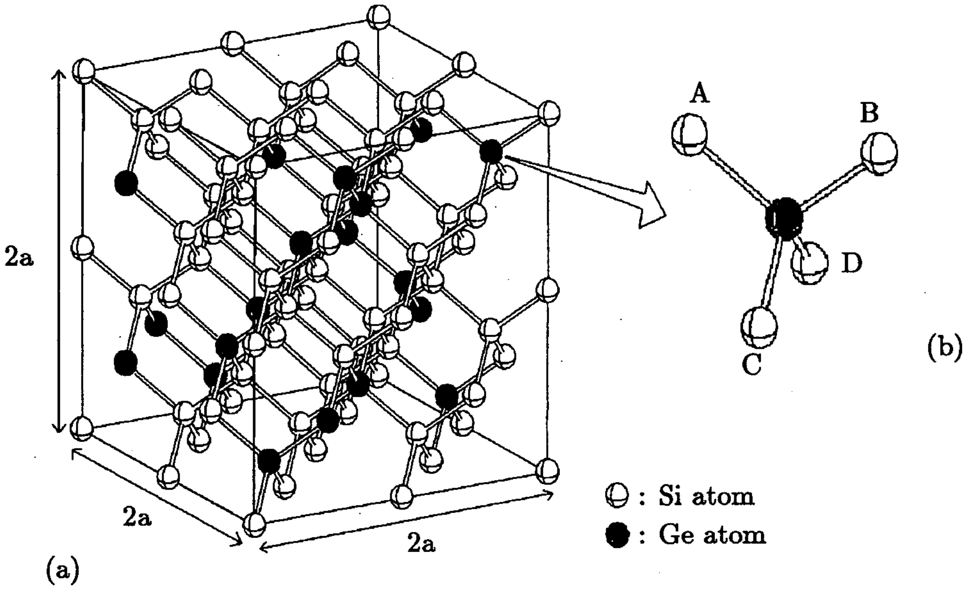

Figure 3: (a) The ball-and-stick model including 64 atoms in the unit cell together with some atoms near boundary of the neighbor cell. The composition of Ge content x is 0.25. (b) The enlarged view of a Ge atom and nearest neighbor Si atoms from (a).

We calculated the relaxed structures by minimizing the total energy of various configurations using steepest descent method. The steepest descent calculation was performed after an annealing process for 1000 MD steps with starting temperature at 500 K. This process is shown in Fig. 2.

Figure 3(a) shows an example of a configuration of the system with x=0.25. There are 64 atoms in the unit cell, (48 atoms of Si and 16 atoms of Ge). In the initial configuration, all atoms are located at the diamond lattice sites with bond length 2.3725 Å which is calculated by the average between Si-Si (2.35 Å) and Ge-Ge (2.44 Å) bond length with ratio x of Ge-Ge.

After relaxation, bond lengths between a Ge atom and its neighboring atoms A, B, C, D in Fig. 3(b), for example, are 2.387 Å, 2.387 Å, 2.382 Å and 2.386 Å, respectively. In average, each Si-Ge bond length stretches about 0.6 %, and Ge-Ge bond length stretches about 1.7 %. On the contrary, Si-Si bond length shortens about 0.5 %. Because the bulk Si crystal is stable with bond length 2.35 Å and Ge crystal with 2.44 Å, Si-Si bond length tends to shorten and Ge-Ge bond length tends to stretch to reach for a stable configuration. In the case of Si-Ge bond length, it stretches when Si content is more than Ge content ($x < 0.5$) and shortens when Si content is less than Ge content ($x > 0.5$).

3.2 Elastic Properties

In this section, we discuss the mechanical properties of $\mathrm{Si}_{1-x}\mathrm{Ge}_x$ alloys from the results on the TB calculations of elastic constants (bulk modulus B, elastic constants C_{11}, C_{12} and C_{44}).

For these calculations, we use a unit cell with only eight atoms. We have confirmed that the results with 64 atoms cell gave essentially the same values of elastic constants. The number of k-points sampled in these calculations is 216 on a dense, regular mesh points in the Brillouin zone.

Figure 4 shows, the total energy as a function of strain for bulk Ge (x=1) as an example. From these energy-strain curves, the equilibrium lattice constants and the elastic constants are

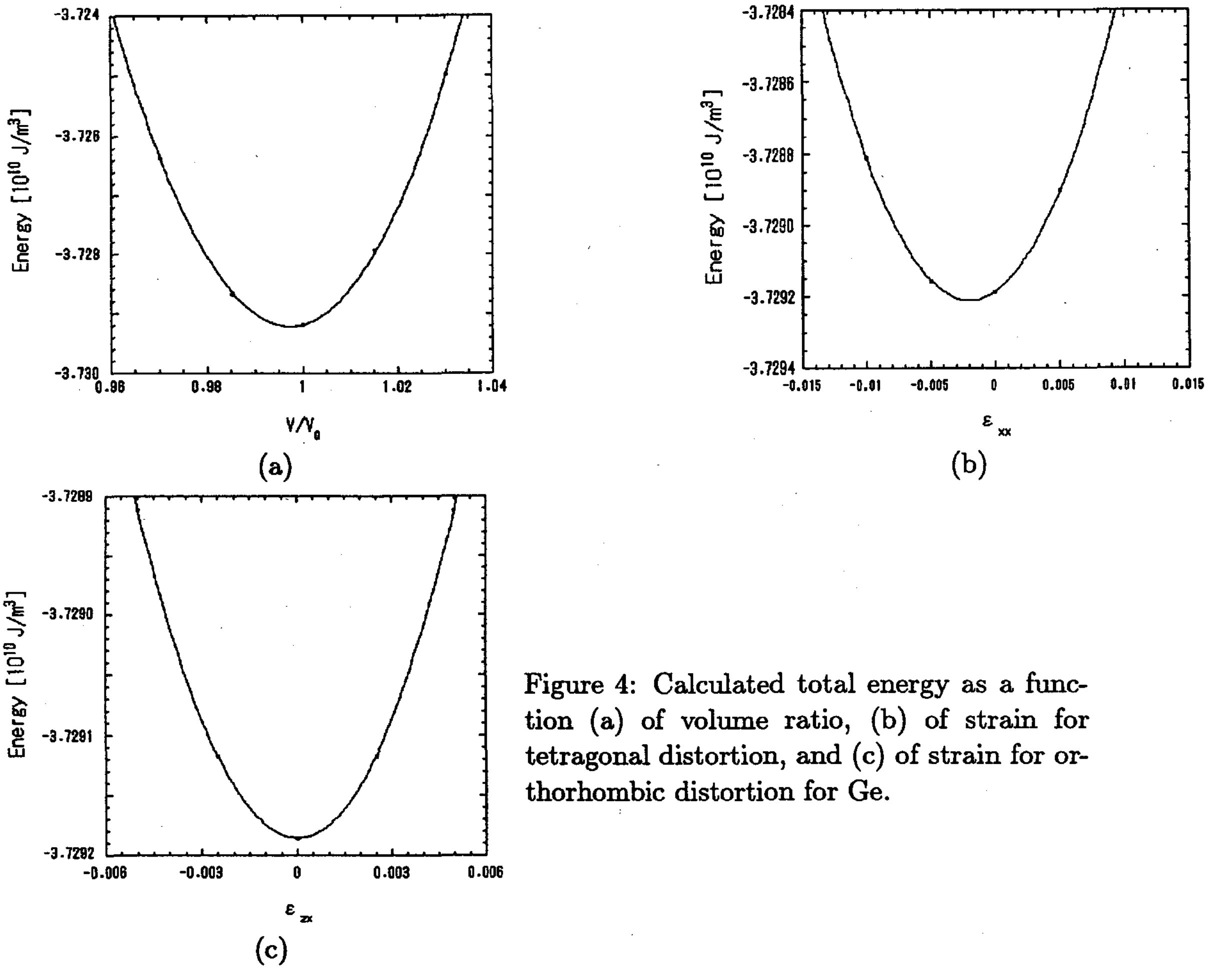

(a)

(b)

(c)

Figure 4: Calculated total energy as a function (a) of volume ratio, (b) of strain for tetragonal distortion, and (c) of strain for orthorhombic distortion for Ge.

obtained for each configuration. We present the dependence of elastic constants upon Ge content x in Fig. 5. We plot the averaged values calculated over various configurations at a given x.

Figure 5 shows that the Si crystal is harder than the Ge crystal, and the alloy becomes softer as the Ge content x increases. At each x, the moduli are calculated for several initial configurations, and the lines in Fig. 5 are drawn on the averaged points over these configurations. We thus obtain monotonic variation of the moduli as a functions of x.

Table 2 lists comparisons between the elastic constants obtained by the present model and those obtained by experiments [10]. In addition, we compare our results with the experimental data [11] and theoretical data [12] of shear modulus for Si/Ge superlattices. The comparison shows an agreement of the monotonic dependence of the elastic constants on x. Theoretical values of the elastic constants of $Si_{0.5}Ge_{0.5}$ zinc blende alloy in Ref. [13] agree also with our results.

We show the equilibrium lattice constant as a function of x in Fig. 6. First-principle calculations [13] and experimental data [14] on the lattice constant compare favorably with our results. From the above comparisons of Si, Ge and $Si_{0.5}Ge_{0.5}$ zinc-blende alloy and the tendency of elastic property in the superlattice, we suppose the present TB model gives reasonable results in the elastic properties of SiGe alloys.

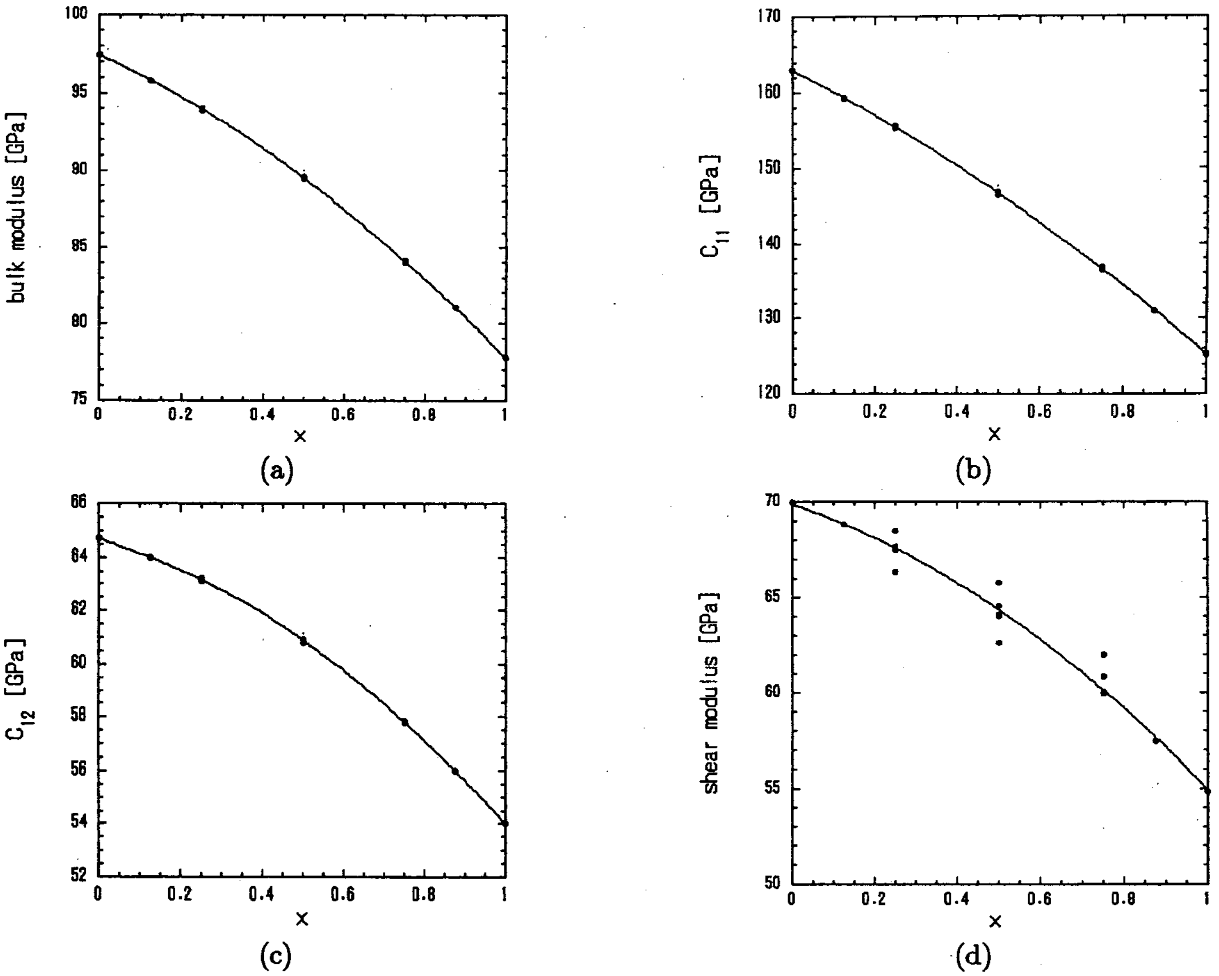

(a) (b) (c) (d)

Figure 5: Dependence of elastic constants upon Ge content x; (a) bulk modulus B, (b) C_{11}, (c) C_{12}, (d) C_{44}. (Lines are only to guide the eye.)

Table 2: Comparison of elastic constants between the present calculation and experimental data [10]. (Unit is GPa.)

	calculation		experiment	
	Si	Ge	Si	Ge
B	97.5	77.7	98.8	77.2
C_{11}	163.0	125.2	166.0	128.5
C_{12}	64.7	54.0	63.9	48.3
C_{44}	70.0	54.8	79.6	68.0

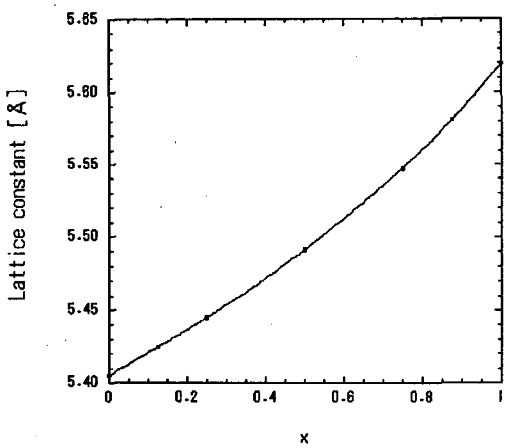

Figure 6: Dependence of equilibrium lattice constant upon Ge content x.

4 CONCLUSION

We have presented the tight-binding molecular dynamics method including nonorthogonality of the atomic orbitals. We have calculated the electronic structure, equilibrium volume and elastic properties of $Si_{1-x}Ge_x$ alloys, and analyzed change of bond length and bond angles in the relaxed configurations.

The elastic constants (B, C_{11}, C_{12} and C_{44}) of $Si_{1-x}Ge_x$ alloys decrease smoothly from Si (x=0) to Ge (x=1) with the increase of Ge content x. These results are compared favorably with other works.

The TBMD study on elastic properties and electronic structures of SiGe superlattices is in progress.

References

[1] W. A. Harrison, *Electronic Structure and the Properties of Solids*, (Freeman, San Francisco, 1980).

[2] M. Menon and K. R. Subbaswamy, Phys. Rev. B **47**, 12754 (1993).

[3] P. Ordejón, D. Lebedenko and M. Menon, Phys. Rev. B **50**, 5645 (1994).

[4] M. Menon and K. R. Subbaswamy, Phys. Rev. B **50**, 11577 (1994).

[5] M. Menon and K. R. Subbaswamy, Phys. Rev. B **55**, 9231 (1997).

[6] M. Menon, J. Phys: Condensed Matter **10**, 10991 (1998).

[7] N. Bernstein and E. Kaxiras, Mater. Res. Sec. Symp. Proc. **408**, 55 (1996).

[8] N. Bernstein and E. Kaxiras, Phys. Rev. B **56**, 10488 (1997).

[9] R. Hoffmann, J. Chem. Phys. **39**, 1397 (1963).

[10] C. Kittel, *Introduction to Solid State Physics*, (Wiley, New York, 1996).

[11] A. de Bernabé, R. Jiménez, M. García-Hernández and C. Prieto, Thin Solid Films **317**, 255 (1998).

[12] M. Grimsditch and F. Nizzoli, Phys. Rev. B **33**, 5891 (1986).

[13] A. Qteish and R. Resta, Phys. Rev. B **37**, 1308 (1988).

[14] J. P. Dismukes, L. Ekstrom and R. J. Paff, J. Phys. Chem. **68**, 3021 (1964).

[15] J. C. Slater and G. F. Koster, Phys. Rev. **94**, 1498 (1954).

[16] L. D. Landau and E. M. Lifshitz, *Theory of Elasticity*, (Perganon, New York, 1986).

[17] D. Itova, N. Kioussis and S. P. Lim, Phys. Rev. B **54**, 14413 (1996).

Appendix A. Tight-Binding Method

In tight-binding method, the wave function $\psi_{n\mathbf{k}}(\mathbf{r})$ of valence electrons is approximated by superposition of atomic-like localized orbitals function $\phi_\alpha^{\mathbf{k}}(\mathbf{r})$:

$$\psi_{n\mathbf{k}}(\mathbf{r}) = \sum_{i\alpha} c_{i\alpha}^n \phi_\alpha^{\mathbf{k}}(\mathbf{r} - \mathbf{R}_i), \tag{12}$$

where $\mathbf{R}_i$ is a position vector of ith atom, α is an orbital index, $\mathbf{k}$ is a wave number and n is a band index. The function $\phi_\alpha^{\mathbf{k}}(\mathbf{r})$ is represented by Bloch's summation of a wave function $\varphi_{i\alpha}(\mathbf{r})$ of the orbital α in one atom:

$$\phi_\alpha^{\mathbf{k}}(\mathbf{r} - \mathbf{R}_i) = \frac{1}{\sqrt{N}} \sum_{\mathbf{L}} e^{i\mathbf{k}\cdot(\mathbf{R}_i + \mathbf{L})} \varphi_{i\alpha}(\mathbf{r} - \mathbf{R}_i - \mathbf{L}), \tag{13}$$

where N is the number of the unit cell in the system and $\mathbf{L}$ represents the translational vector.

From Eq. (12), (13) and Schrödinger equation

$$H\psi_{n\mathbf{k}}(\mathbf{r}) = E_{n\mathbf{k}}\psi_{n\mathbf{k}}(\mathbf{r}), \tag{14}$$

the following equation is obtained:

$$\sum_{i\alpha}\left(\int \phi_\beta^{\mathbf{k}*}(\mathbf{r} - \mathbf{R}_j) H \phi_\alpha^{\mathbf{k}}(\mathbf{r} - \mathbf{R}_i) d^3r\right) c_{i\alpha}^n = E_{n\mathbf{k}} \sum_{i\alpha} c_{i\alpha}^n \int \phi_\beta^{\mathbf{k}*}(\mathbf{r} - \mathbf{R}_j) \phi_\alpha^{\mathbf{k}}(\mathbf{r} - \mathbf{R}_i) d^3r. \tag{15}$$

In Eq. (15), orthogonal matrix element $H_{\alpha\beta}$ and nonorthogonal matrix element $S_{\alpha\beta}$ are defined respectively by

$$\begin{aligned} H_{\alpha\beta}^{\mathbf{k}}(\mathbf{R}_i - \mathbf{R}_j) &= \int \phi_\beta^{\mathbf{k}*}(\mathbf{r} - \mathbf{R}_j) H \phi_\alpha^{\mathbf{k}}(\mathbf{r} - \mathbf{R}_i) d^3r \\ &= \sum_{\mathbf{L}} e^{i\mathbf{k}\cdot(\mathbf{R}_i - \mathbf{R}_j - \mathbf{L})} \int \varphi_{j\beta}{}^*(\mathbf{r} - \mathbf{R}_j) H \varphi_{i\alpha}(\mathbf{r} - \mathbf{R}_i - \mathbf{L}) d^3r, \qquad (16) \\ S_{\alpha\beta}^{\mathbf{k}}(\mathbf{R}_i - \mathbf{R}_j) &= \int \phi_{\mathbf{k}}{}^{\beta*}(\mathbf{r} - \mathbf{R}_j) \phi_{\mathbf{k}}{}^{\alpha}(\mathbf{r} - \mathbf{R}_i) d^3r \\ &= \sum_{\mathbf{L}} e^{i\mathbf{k}\cdot(\mathbf{R}_i - \mathbf{R}_j - \mathbf{L})} \int \varphi_{j\beta}{}^*(\mathbf{r} - \mathbf{R}_j) \varphi_{i\alpha}(\mathbf{r} - \mathbf{R}_i - \mathbf{L}) d^3r. \qquad (17) \end{aligned}$$

Here, orbitals on the same atom are assumed to be orthogonal to one another, but orbitals on different atoms are not necessarily orthogonal.

Thus these equations are reduced to the generalized eigenvalue problem:

$$\mathbf{HC}^n = E_n \mathbf{SC}^n, \tag{18}$$

where $\mathbf{H}$ is an orthogonal Hamiltonian matrix, $\mathbf{S}$ is a nonorthogonal overlap matrix, E_n is an eigenvalue and $\mathbf{C}^n$ is an eigenvector.

Using Slater-Koster formulation [15], the orthogonal energy elements between each orbitals (s-s, s-p_k, p_k-s, p_k-p_k, p_k-$p_{k'}$, k and $k' = x, y, z$) are obtained as follows:

$$E_{ss}(\mathbf{r}) = V_{ss\sigma}(\mathbf{r}), \tag{19}$$

$$E_{sp_x}(\mathbf{r}) = V_{sp\sigma}(\mathbf{r})\frac{x}{r}, \quad E_{sp_y} = (x \leftrightarrow y), \quad E_{sp_z} = (x \leftrightarrow z), \tag{20}$$

$$E_{p_xs}(\mathbf{r}) = -V_{sp\sigma}(\mathbf{r})\frac{x}{r}, \quad E_{p_ys} = (x \leftrightarrow y), \quad E_{p_zs} = (x \leftrightarrow z), \tag{21}$$

$$\begin{aligned}
&E_{p_xp_x}(\mathbf{r}) = V_{pp\sigma}(\mathbf{r})\left(\frac{x}{r}\right)^2 + V_{pp\pi}(\mathbf{r})\left\{1-\left(\frac{x}{r}\right)^2\right\}, \\
&E_{p_yp_y} = (x \leftrightarrow y), \quad E_{p_zp_z} = (x \leftrightarrow z), && (22)\\
&E_{p_xp_y}(\mathbf{r}) = V_{pp\sigma}(\mathbf{r})\frac{x}{r}\frac{y}{r} - V_{pp\pi}(\mathbf{r})\frac{x}{r}\frac{y}{r}, \\
&E_{p_yp_z} = (x \leftrightarrow y, y \leftrightarrow z), \quad E_{p_zp_x} = (x \leftrightarrow z, y \leftrightarrow x). && (23)
\end{aligned}$$

The Hamiltonian matrix $\mathbf{H}$ is written by

$$H^{\mathbf{k}}_{i\alpha j\beta} = \sum_{\mathbf{L}} e^{i\mathbf{k}\cdot(\mathbf{r}-\mathbf{L})} E_{i\alpha j\beta}\left(1+\frac{1}{K}-T_2{}^2\right). \tag{24}$$

The nonorthogonal energy elements $T_{i\alpha j\beta}$ are also obtained by replacing $V_{\lambda\lambda'\mu}(\mathbf{r})$ with $T_{\lambda\lambda'\mu}(\mathbf{r})$ in the above formulae. The overlap matrix $\mathbf{S}$ is written by

$$S^{\mathbf{k}}_{i\alpha j\beta} = \sum_{\mathbf{L}} e^{i\mathbf{k}\cdot(\mathbf{r}-\mathbf{L})} T_{i\alpha j\beta}. \tag{25}$$

Appendix B. The Hellmann-Feynman Theorem

We derive the Hellmann-Feynman theorem [2] for the present formulation: In matrix form Eq. (18) becomes

$$(\mathbf{H} - E_n\mathbf{S})\mathbf{C}^n = \mathbf{0}, \tag{26}$$

where $\mathbf{C}^n$ is a column vector. Taking the Hermitian conjugate ,

$$\mathbf{C}^{n\dagger}(\mathbf{H} - E_n\mathbf{S}) = \mathbf{0}, \tag{27}$$

where $\mathbf{H}$ and $\mathbf{S}$ are Hermitian. Differentiating Eq. (26) with respect to $\mathbf{r}$, we obtain

$$\left[\frac{\partial}{\partial\mathbf{r}}(\mathbf{H} - E_n\mathbf{S})\right]\mathbf{C}^n + (\mathbf{H} - E_n\mathbf{S})\frac{\partial}{\partial\mathbf{r}}\mathbf{C}^n = \mathbf{0}. \tag{28}$$

Multiplying on the left with $\mathbf{C}^{n\dagger}$ and using Eq. (27), we have

$$\mathbf{C}^{n\dagger}\left[\frac{\partial}{\partial\mathbf{r}}(\mathbf{H} - E_n\mathbf{S})\right]\mathbf{C}^n = \mathbf{0}. \tag{29}$$

From these equations we finally obtain

$$\frac{\partial E_n}{\partial\mathbf{r}} = \frac{\mathbf{C}^{n\dagger}\left(\frac{\partial\mathbf{H}}{\partial\mathbf{r}} - E_n\frac{\partial\mathbf{S}}{\partial\mathbf{r}}\right)\mathbf{C}^n}{\mathbf{C}^{n\dagger}\mathbf{S}\mathbf{C}^n}. \tag{30}$$

The $\mathbf{C}^n$ is normalized so that

$$\mathbf{C}^{n\dagger}\mathbf{S}\mathbf{C}^n = 1. \tag{31}$$

It is thus necessary to have analytical form of $\frac{\partial\mathbf{H}}{\partial\mathbf{r}}$ and $\frac{\partial\mathbf{S}}{\partial\mathbf{r}}$. From Eq. (1), we have

$$\frac{\partial V_{\lambda\lambda'\mu}(\mathbf{r})}{\partial x} = -\frac{\alpha x}{r}V_{\lambda\lambda'\mu}(\mathbf{r}). \tag{32}$$

From Eq. (19)~(23), $\frac{\partial E_{i\alpha j\beta}}{\partial x}$ is given by

$$\begin{aligned}
\frac{\partial E_{ss}(\mathbf{r})}{\partial x} &= \frac{\partial V_{ss\sigma}(\mathbf{r})}{\partial x}, && (33)\\
\frac{\partial E_{sp_x}(\mathbf{r})}{\partial x} &= \frac{\partial V_{sp\sigma}(\mathbf{r})}{\partial x}\frac{x}{r} + V_{sp\sigma}(\mathbf{r})\left(\frac{1}{r} - \frac{x^2}{r^3}\right), && (34)\\
\frac{\partial E_{sp_y}(\mathbf{r})}{\partial x} &= \frac{\partial V_{sp\sigma}(\mathbf{r})}{\partial x}\frac{y}{r} - V_{sp\sigma}(\mathbf{r})\frac{xy}{r^3}, \quad \frac{\partial E_{sp_z}(\mathbf{r})}{\partial x} = (y \leftrightarrow z), && (35)\\
\frac{\partial E_{p_xp_x}(\mathbf{r})}{\partial x} &= \frac{\partial V_{pp\sigma}(\mathbf{r})}{\partial x}\frac{x^2}{r^2} + \frac{\partial V_{pp\pi}(\mathbf{r})}{\partial x}\left(1 - \frac{x^2}{r^2}\right) + (V_{pp\sigma}(\mathbf{r}) - V_{pp\pi}(\mathbf{r}))\frac{2x(r^2 - x^2)}{r^4}, && (36)\\
\frac{\partial E_{p_yp_y}(\mathbf{r})}{\partial x} &= \frac{\partial V_{pp\sigma}(\mathbf{r})}{\partial x}\frac{y^2}{r^2} + \frac{\partial V_{pp\pi}(\mathbf{r})}{\partial x}\left(1 - \frac{y^2}{r^2}\right) - (V_{pp\sigma}(\mathbf{r}) - V_{pp\pi}(\mathbf{r}))\frac{2xy^2}{r^4}, && \\
\frac{\partial E_{p_zp_z}(\mathbf{r})}{\partial x} &= (y \leftrightarrow z), && (37)\\
\frac{\partial E_{p_xp_y}(\mathbf{r})}{\partial x} &= \left(\frac{\partial V_{pp\sigma}(\mathbf{r})}{\partial x} - \frac{\partial V_{pp\pi}(\mathbf{r})}{\partial x}\right)\frac{xy}{r^2} + (V_{pp\sigma}(\mathbf{r}) - V_{pp\pi}(\mathbf{r}))\left(1 - \frac{2x^2}{r^2}\right)\frac{y}{r^2}, && \\
\frac{\partial E_{p_zp_x}(\mathbf{r})}{\partial x} &= (y \leftrightarrow z), && (38)\\
\frac{\partial E_{p_yp_z}(\mathbf{r})}{\partial x} &= \left(\frac{\partial V_{pp\sigma}(\mathbf{r})}{\partial x} - \frac{\partial V_{pp\pi}(\mathbf{r})}{\partial x}\right)\frac{yz}{r^2} - (V_{pp\sigma}(\mathbf{r}) - V_{pp\pi}(\mathbf{r}))\frac{2xyz}{r^4}. && (39)
\end{aligned}$$

From Eq. (2), we obtain

$$\frac{\partial T_{\lambda\lambda'\mu}(\mathbf{r})}{\partial x} = \frac{2}{\varepsilon_\lambda + \varepsilon_{\lambda'}}\left\{\frac{1}{K(\mathbf{r})}\frac{\partial V_{\lambda\lambda'\mu}(\mathbf{r})}{\partial x} + V_{\lambda\lambda'\mu}(\mathbf{r})\frac{\partial}{\partial x}\left(\frac{1}{K(\mathbf{r})}\right)\right\}, \tag{40}$$

where

$$\frac{\partial}{\partial x}\left(\frac{1}{K(\mathbf{r})}\right) = -2\sigma(r - d_0)\frac{x}{r}\frac{1}{K(\mathbf{r})}. \tag{41}$$

From Eq. (24), the derivative of **H** can be calculated as

$$\frac{\partial H^{\mathbf{k}}_{i\alpha j\beta}}{\partial x} = \\
\sum_{\mathbf{L}} e^{i\mathbf{k}\cdot(\mathbf{r}-\mathbf{L})}\left\{\left(\frac{\partial E_{i\alpha j\beta}}{\partial x} + ik_x E_{i\alpha j\beta}\right)\left(1 + \frac{1}{K(\mathbf{r})} - {T_2}^2\right) + E_{i\alpha j\beta}\frac{\partial}{\partial x}\left(1 + \frac{1}{K(\mathbf{r})} - {T_2}^2\right)\right\}, \tag{42}$$

where

$$\frac{\partial}{\partial x}\left(1 + \frac{1}{K(\mathbf{r})} - {T_2}^2\right) = \frac{\partial}{\partial x}\left(\frac{1}{K(\mathbf{r})}\right) - \frac{T_2}{2}\left(\frac{\partial T_{ss\sigma}(\mathbf{r})}{\partial x} - 2\sqrt{3}\frac{\partial T_{sp\sigma}(\mathbf{r})}{\partial x} - 3\frac{\partial T_{pp\sigma}(\mathbf{r})}{\partial x}\right). \tag{43}$$

And from Eq. (25), $\frac{\partial \mathbf{S}}{\partial x}$ can be calculated as

$$\frac{\partial S^{\mathbf{k}}_{i\alpha j\beta}}{\partial x} = \sum_{\mathbf{L}} e^{i\mathbf{k}\cdot(\mathbf{r}-\mathbf{L})}\left(\frac{\partial T_{i\alpha j\beta}}{\partial x} + ik_x T_{i\alpha j\beta}\right). \tag{44}$$

Appendix C. Elastic Constants

The elastic constants C_{ij} can be calculated from the Taylor expansion of the total energy of the system, $E(V,\varepsilon)$, with respect to a small strain ε of the lattice (V is the volume of the system) [16][17]. The Taylor expansion of the total energy at an equilibrium volume, V_0, can be written as

$$E(V,\varepsilon_i) = E(V_0,0) + \frac{V_0}{2}\sum_{i,j} C_{ij}\varepsilon_i\varepsilon_j + O[\varepsilon_i^3], \tag{45}$$

where $O[\varepsilon_i^3]$ indicates that the neglected terms in the polynomial expansion are third and a higher order of ε_i. There are 21 independent elastic constants C_{ij} in Eq. (45). Symmetry reduces this number to three (C_{11}, C_{12} and C_{44}) for the cubic lattices.

The TBMD method is employed to determine $E(V,\varepsilon)$ for various strains. The elastic constants are then obtained from the curvatures of the total energy-strain curves. Bulk modulus is obtained by

$$B = V_0\left(\frac{d^2E}{dV^2}\right)_{V=V_0}. \tag{46}$$

In this case, the strain matrix elements are $\varepsilon_{xx} = \varepsilon_{yy} = \varepsilon_{zz}$ and $\varepsilon_{yz} = \varepsilon_{zx} = \varepsilon_{xy} = 0$. Calculated total energy as a function of volume ratio V/V_0 is shown in Fig. 4(a) for Ge (content x is 1) as an example. Next in the case of C_{11}, the energy function of ε_{xx} is plotted in Fig. 4(b). Here the strain matrix elements are $\varepsilon_{yy} = \varepsilon_{zz} = \varepsilon_{yz} = \varepsilon_{zx} = \varepsilon_{xy} = 0$. Pure-shear modulus C_{44} is obtained from the energy curve as a function of ε_{zx} shown in Fig. 4(c). Here the strain matrix elements are $\varepsilon_{xx} = \varepsilon_{yy} = \varepsilon_{zz} = \varepsilon_{yz} = \varepsilon_{xy} = 0$.

For cubic systems, the bulk modulus B is related to the elastic constants by

$$B = \frac{C_{11} + 2C_{12}}{3}. \tag{47}$$

In the present study we obtain C_{12} from Eq. (47) by calculating B and C_{11}.